23 July 1965, Volume 149, Number 3682 SCIENCE

Tracks of Charged Particles in Solids

These tracks are becoming useful tools in many fields of science and engineering.

R. L. Fleischer, P. B. Price, R. M. Walker

Almost all insulating solids, including natural minerals, glasses, and plastics, record tracks of nuclear charged particles. In this article, after first describing the nature of tracks in solids and ways of seeing them, we show how they have been used in such diverse problems as measuring the age of geological and archeological specimens, studying the early history of the solar system recorded in meteorites, observing nuclear interactions, determining neutron fluxes, and separating biological cells of different sizes.

Nature of Tracks in Solids

In most ordinary insulating solids, massive energetic charged particles produce narrow trails of damage—or tracks—that can be seen by means of various magnification schemes. The most direct method, and the one first used by Silk and Barnes (*1*) to discover particle tracks in solids, is to examine the irradiated solid with an electron microscope at very high magnification. Figure 1, for example, shows a transmission electron micrograph of tracks in a thin crystal of zircon ($ZrSiO_4$) that has been irradiated with uranium fission fragments (*2*). The tracks are visible because the diffraction contrast has been locally altered by the production of damaged, strained regions around the paths of the bombarding fission fragments.

Although tracks have been seen by means of electron diffraction contrast in a number of materials (*1*, *3*), the procedure is cumbersome, requiring the preparation of extremely thin samples ($\lesssim$ 3000 Å), and can be used only with great difficulty for most solids. Even with suitable solids, the high magnification needed to see the tracks requires that track densities be high in order for studies to be possible. Finally, only a small portion of the total range of most heavy particles of interest can be examined at one time in the electron microscope.

Fortunately, there is another, much more general method (*4*) of revealing tracks which is applicable to many solids (*4*–*7*) and permits study of tracks in the optical microscope (*8*), where low densities of tracks and total ranges can be easily measured. Very early in our work we found that damage trails made by charged particles can be chemically attacked much more rapidly than the normal, undamaged regions of a sample. Mica, in which this effect was first discovered (*4*), presents an especially simple example of track revelation by preferential attack. When a sample of mica containing charged-particle tracks is placed in hydrofluoric acid, the acid rapidly penetrates the full length of the tracks, replacing the linear trails of damaged material with fine hollow tubes ~50 Å in diameter. These tubes are permanent features of the sample and greatly facilitate the study of tracks in the electron microscope. More importantly, continued chemical attack makes it possible to see the tracks in an optical microscope (*8*). The etching increases the diameter of the hollow tubes, so that when they reach a diameter comparable to the wavelength of visible light they become visible in the optical microscope, appearing black in normal bright-field illumination and white when viewed in dark field (*9*).

In some materials, such as muscovite mica, zircon, and diopside, the rate at which the holes widen is much less rapid than the rate at which the damaged material is attacked, with the result that the etched tracks are of constant diameter. In other materials (glass is a good example) the rate of attack along the radiation-damaged regions is greater than, but comparable to, the overall attack rate, so that the etched tracks are tapered rather than cylindrical. In extreme cases, as in the etching of calcite or lithium fluoride (*10*), only shallow etch pits result. Etched tracks in different materials are shown in Fig. 2 (*11*).

The geometry of etched tracks varies with the substance being examined, the solvents used, and the time and temperature of attack. There are only general guidelines to aid the experimenter in choosing the proper etching conditions for track development, and any new substance must still be approached empirically (*5*). The important thing to realize, however, is that the preferential revelation of tracks is a very general phenomenon. In most insulating substances—minerals (*5*), glasses (*6*), or polymers (*7*)—it has been possible to reveal charged-particle tracks. Thus, almost any insulator can now be used as a charged-particle track detector.

Another method of revealing tracks is by decoration—preferential forma-

The authors are affiliated with the General Electric Research Laboratory, Schenectady, New York.

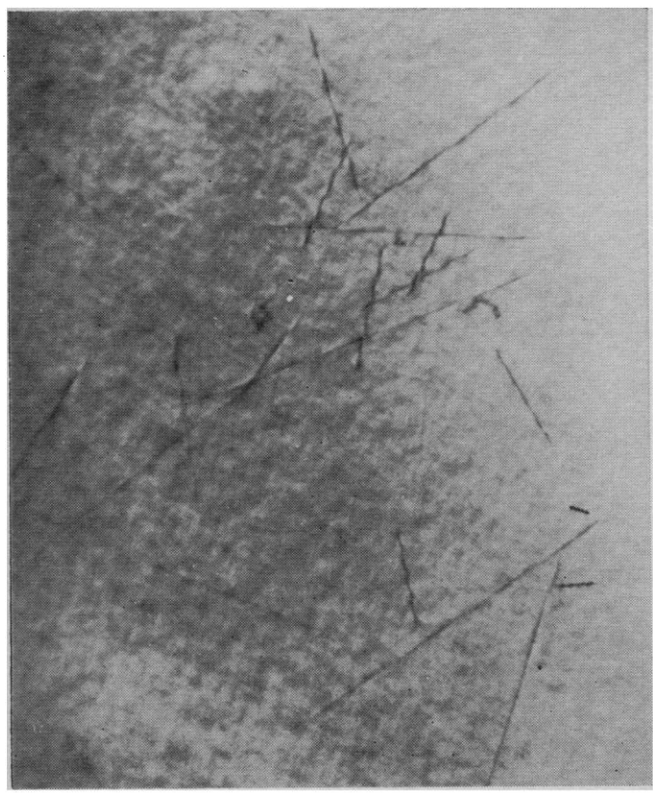

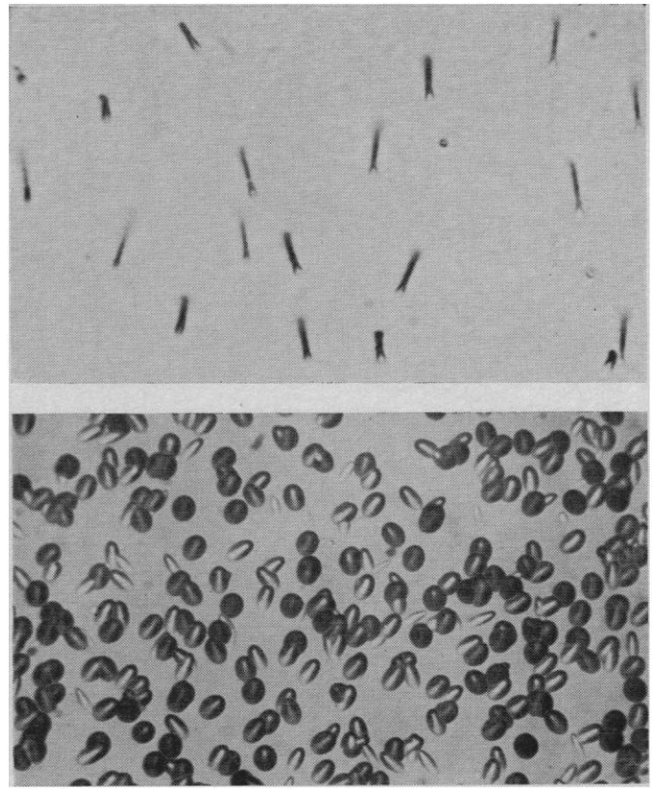

Fig. 1 (left). Fission-fragment tracks in zircon, as viewed by transmission electron microscopy. The tracks appear as black diffraction contrast lines (see *2*). (× 50,000) Fig. 2. (Top right) Tracks of 3-Mev alpha particles in cellulose nitrate, etched 2 hours in 6*N* NaOH solution at 20°C (× 1000) (Bottom right) Fission-fragment tracks in soda glass, etched 10 seconds in 48-percent hydrofluoric acid. (× 1500)

tion of a visible second-phase material at the radiation-damage regions. This is, of course, the classic method of track development in photographic emulsions. The decoration technique has recently been extended to single crystals of silver chloride, by Childs and Slifkin (*12*), and has also been demonstrated by us in a sample of silver-doped glass (*6*). Although this method of revealing tracks is potentially powerful, it has not yet proved applicable to most solids, and here we concern ourselves only with the chemical etching method of track revelation.

To explore the utility of solid-state track detectors in nuclear physics and other areas, it is essential to know the sensitivity of the substance for particle-track registration. By using different particles at various energies we have shown that the response of any substance to charged particles is determined by a single parameter, the critical rate of energy loss for track formation, $(dE/dx)_c$ (*13*). Knowing the value of $(dE/dx)_c$ for any substance, we can predict which particles will register tracks, and at what energies.

In Fig. 3, from work done with E. L. Hubbard of the heavy-ion accelerator staff at the Lawrence Radiation Laboratory (*13*), we show the results which led to the conclusion that the response of various solids can indeed be characterized by $(dE/dx)_c$. In Fig. 3 (top) the solid lines are theoretical curves of the rate of energy loss as a function of energy, plotted for various heavy ions. The points represent mica-irradiation experiments in which we searched for tracks after bombardment. The letters beside the dots indicate whether we found long tracks (*L*), no tracks (*N*), or partial track development (*P*). It may be seen that when dE/dx is sufficiently high, long tracks are formed with a 1-to-1 correspondence between incident particles and tracks. When (dE/dx) falls too low, no tracks are seen. The transition region, where partial development is observed, is remarkably narrow. Figure 3 (bottom) shows the appearance in mica of argon ion tracks with $dE/dx > (dE/dx)_c$.

Because the maximum possible value of dE/dx increases with increasing atomic number, the existence of a critical dE/dx means that for every substance there is a lower limit for the masses of heavy ions which can produce tracks. Thus, in mica, tracks of particles lighter than silicon can *never* be etched out, regardless of their energy. Fortunately, different substances have widely different values of $(dE/dx)_c$, thereby making it possible to choose detectors which will differentiate between particles of different mass.

Sensitivity differences between two materials are illustrated in Fig. 4, which shows three samples which were simultaneously exposed to a beam of 3-Gev protons from the Brookhaven Cosmotron. Pure mica, shown in Fig. 4 (left), contains only an occasional etched track, produced by the interaction of the incident protons with heavy-element impurities. As Fig. 4 (middle) shows, when a thin (~50-Å) layer of lead is placed next to mica, the track density is drastically increased; the long tracks represent proton-induced fissions of lead, and the short tracks represent spallation reactions with lead nuclei. Figure 4 (right) shows a sample of Lexan polycarbonate exposed to the same beam. Here the proton-induced recoils in the plastic itself are visible, and the sample contains too many tracks to be usable. An even more sensitive substance than Lexan is cellulose nitrate [see Fig. 2 (top)], which registers tracks of particles as light as deuterons (*14*).

Table 1 summarizes the values of $(dE/dx)_c$ found for various solids.

For geological applications it is particularly important to know the length of time that tracks are stable at different temperatures. We have investigated this question by heating track-containing samples of various materials until the tracks begin to disappear. The kinetics of track fading are characterized by activation energies ranging from 1 to 9 electron volts (*15*, *16*), the higher values being for substances in which the tracks should be stable for geologic times even at temperatures as high as 600°C. Other experiments have shown that the sensitivity for track registration remains unchanged for sample temperatures ranging from 77°K up to the temperatures at which tracks are no longer stable (*16*). Finally, we have demonstrated that neither high pressures (~80 kilobars) nor large doses of ionizing radiation affect either the formation or the retention of tracks in crystalline materials (*16*). Thus, tracks can be formed in a wide variety of substances over a wide range of environmental conditions and they will remain for long times.

The basic radiation-damage mechanism which produces the latent image of the track in solids has been previously attributed to either "displacement spikes" (*17*) or "thermal spikes" (*18*). While these mechanisms may possibly give rise to tracks in certain solids, we believe that in the vast majority of cases neither of these mechanisms is primarily responsible for the tracks that we see. One of the most striking characteristics of track-registering materials is the correlation with their electrical conductivity (*19*). Insulators and certain semiconducting glasses may register tracks; metals and the better semiconductors, such as silicon and germanium, do not. We have developed a model of track formation—the ion-explosion spike—that explains this dependence on conductivity and accounts for the observed sequence of sensitivities shown in Table 1 (*19*). The model approximately predicts the observed track dimensions and the absolute values of $(dE/dx)_c$. The fundamental idea is that a continuous, cylindrical region of damage may be created by the violent coulombic repulsion of the positive ions remaining after the scattering away of electrons by an energetic, massively charged particle. The proposed mechanism is shown schematically in Fig. 5.

Nuclear Physics

Several factors make solid-state track detectors uniquely useful and flexible tools for nuclear physics research. These are: (i) their ability to withstand, without fading or fogging, enormous doses of particles whose rates of energy loss are less than the critical value $(dE/dx)_c$; (ii) the possibility of choosing either light or heavy target elements, either as constituents of the detector itself or as material placed adjacent to detectors of low

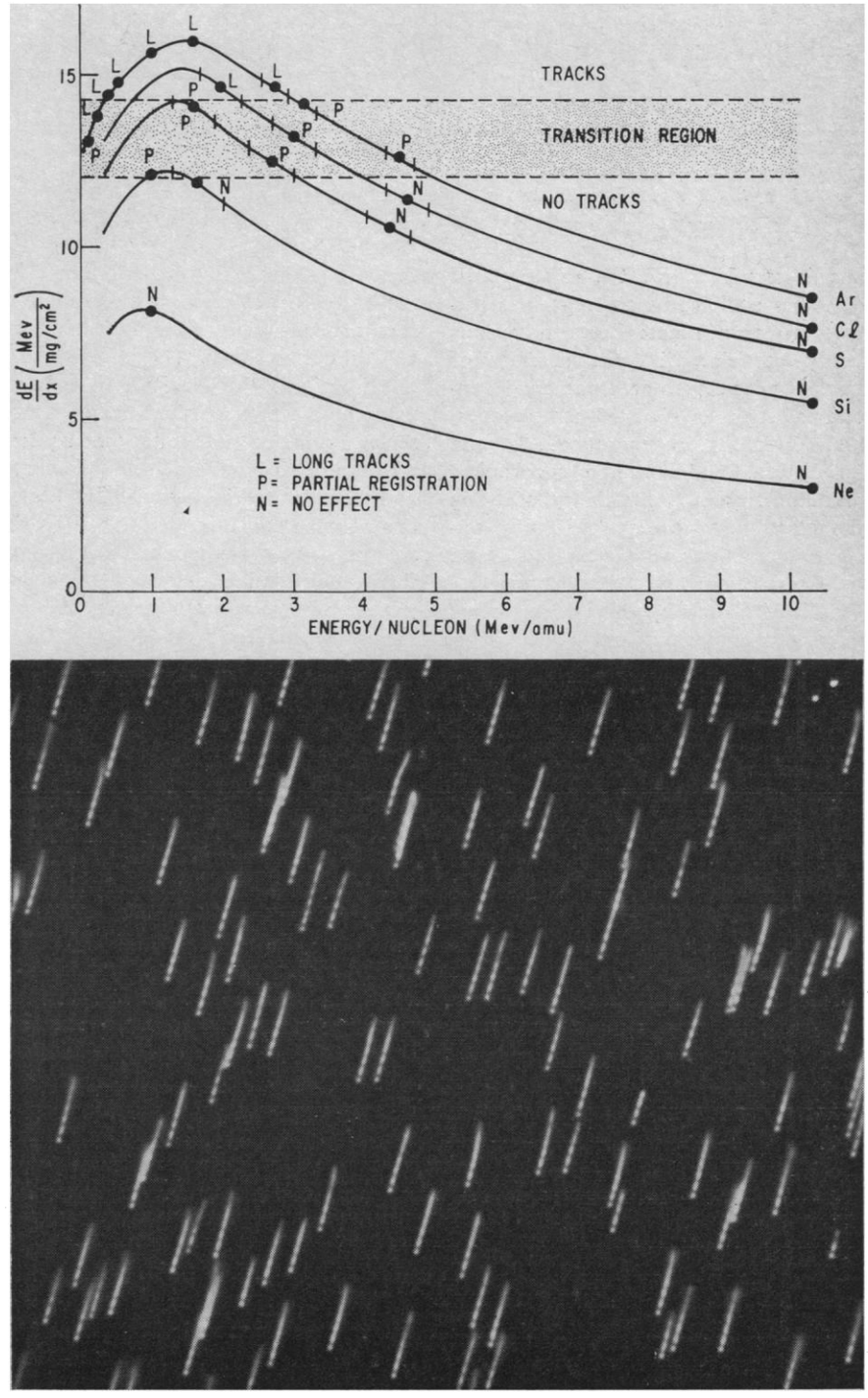

Fig. 3. Track registration in muscovite mica. (Top) The curves show the calculated rates of energy loss of various heavy ions in mica as a function of energy per nucleon. The experimental points indicate registration characteristics which are deduced from experiments such as the one represented by the dark-field photomicrograph (at bottom), which shows etched tracks of 40-Mev argon ions that entered the mica at a 15-degree angle. Impinging particles lighter than silicon cannot be detected and do not impair the ability of mica to detect heavier particles.

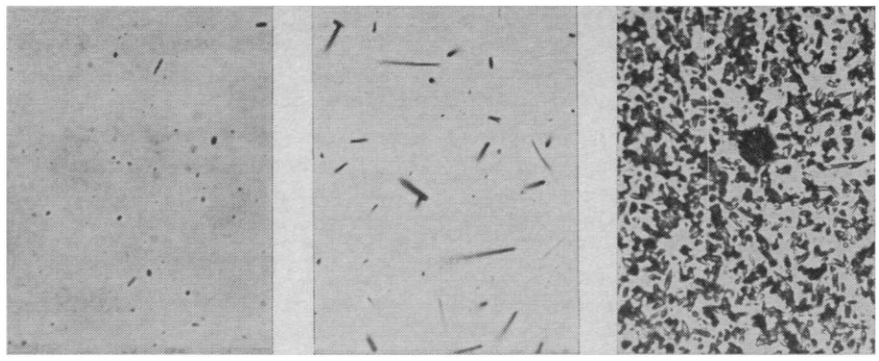

Fig. 4. Tracks induced by exposure to a beam of 3-Gev protons (2×10^{13}/cm^2). (Left) Spallation reactions in muscovite mica. (Middle) Tracks in muscovite mica resulting from fission and spallation reactions in a lead film, 50 Å thick, adjacent to the mica. (Right) Spallation reactions in Lexan polycarbonate resin.

atomic number; (iii) the existence of detectors sufficiently different in sensitivity to discriminate between various heavy particles; (iv) the stability of tracks under severe environmental conditions, such as elevated temperature, high humidity, background β- and γ-radiation, and extreme mechanical vibrations; (v) the possibility of using the electron microscope to study nuclear interactions with high space and time resolution; and (vi) the ease and simplicity of the handling, developing, and observing techniques.

Within the last year, detectors of mica (or glass) have made it possible for the first time to accurately measure the heights of fission barriers of certain heavy elements at the new Berkeley cyclotron (*20*); to verify the existence, and measure the half-life, of an isotope of the newest synthetic element—of atomic number 104—at the heavy-ion cyclotron at Dubna in the U.S.S.R. (*21*); and to measure the spontaneous-fission decay constant of U^{238} in our laboratory (*22*).

Table 1. Sequence of sensitivities of various materials for particle-track registration.

Material	Critical rate of energy loss (Mev/mg cm^2)	Lightest detectable ion	Reference
Pyroxene	~20	Ca	(*19*)
Olivine	~20	Ca	(*19*)
Zircon	~19	Ca	(*19*)
Plagioclase	~19	Ca	(*19*)
Tektite glass	~15	S	(*19*)
Orthoclase and quartz	~15	S	(*19*)
Mica	~13	Si	(*13*)
Polyester resin (Mylar)	~ 4	O	(*19*)
Bisphenol-A polycarbonate resin (Lexan)	~ 4	C	(*13*)
Hydroquinone-bisphenol-A isophthalic terephthalate	~ 3	B	(*19*)
Cellulose acetate butyrate	~ 2	He	(*19*)
Cellulose nitrate	~ 2	H	(*13*)

With E. L. Hubbard, we have been using high-energy particles in the Lawrence Radiation Laboratory heavy-ion accelerator to bombard heavy elements and thereby create unusually heavy compound nuclei, such as $Ar^{40} + Th^{232}$; we then study the modes of decay of these nuclei, using solid-state track detectors. In our most recent experiments we employ synthetic crystals of thorite ($ThSiO_4$) (*23*), whose sensitivity is about the same as that of zircon (Table 1), so that argon ions entering the crystals are not visible and only fissions of the excited compound nuclei produce tracks. Figure 6 is a set of dark-field photomicrographs of fission events which illustrate the two modes of decay we have observed. The V-shaped tracks (Fig. 6*a*) are ordinary binary fissions. The three-pronged tracks (Fig. 6*b*) were observed about 4 percent of the time and are probably due to ternary fissions—events in which the nucleus splits into three heavy fragments of comparable mass. Swiatecki has calculated that a sufficiently highly charged liquid drop will lose more energy by fissioning into three equal fragments than by fissioning into two (*24*), and it appears that our nuclear analog of the highly charged liquid drop—the argon-plus-thorium compound nucleus—breaks into three fragments a significant fraction of the time. The angular distributions of several hundred three-pronged events have now been measured microscopically, and their analysis forms part of the interpretation of the events as ternary fissions (*25*).

The high spatial resolution of the electron microscope makes it an attractive tool for the study of short-time decay events. For example, a typical registerable heavy particle traveling at 10 percent of the speed of light takes only 10^{-16} second to travel the minimum resolution distance of ~30 Å. Although such events have been looked for, none have been found, and this remains an interesting possibility for the future. An example of an experiment in which results were negative is shown in Fig. 7 (top). Two of the tracks in the picture are V-shaped and represent the fission-in-flight of very heavy nuclei produced by the interaction of oxygen ions with lead nuclei in a lead-rich synthetic mica. The absence of any small prongs at the apex of the V's in 1000 such events shows that the probability of forming a product nucleus which fissions in $> 5 \times 10^{-16}$ second is less than 10^{-3}.

Similar V-events are represented in Fig. 7 (bottom), which shows the results of bombarding the same lead-rich mica with 3-Gev protons. These proton-induced events differ qualitatively from the oxygen ion events of Fig. 7 (top) in that, in the proton-induced events, there is marked asymmetry in the widths of the two arms of the V track. This indicates that the fission events induced by heavy ions are more nearly symmetric than are the proton-induced fissions. It further suggests that the widths of the etched tracks provide information about the

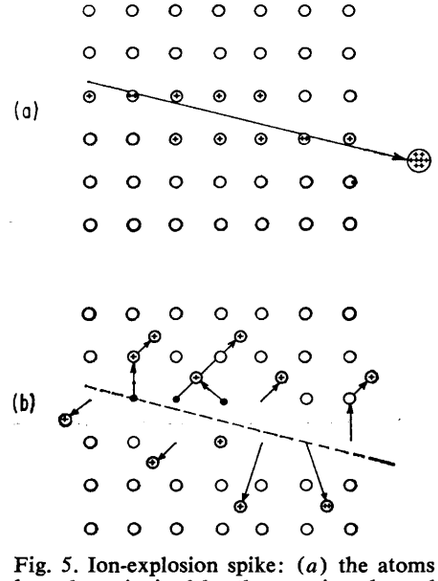

Fig. 5. Ion-explosion spike: (*a*) the atoms have been ionized by the massive charged particle which has just passed; (*b*) the mutual repulsion of the ions has separated them and forced them into the lattice.

absolute value of dE/dx. This important possibility deserves careful future study.

Another advantage of track-registering solids is that they are amenable to automatic scanning procedures. For example, if the detector is sufficiently thin that the tracks go all the way through, the total number of tracks can be deduced by etching for a standard time and measuring the flow of gas or ionic solution through the tracks (*26, 27*).

Activation Analysis and Neutron Dosimetry

The ability of solid-state track detectors to withstand large doses of neutrons and β- and γ-radiation without deterioration makes them uniquely suitable as tools in extremely sensitive microanalyses (*28*) of elements, such as uranium and plutonium, which fission under neutron irradiation, and of elements, such as boron and lithium, which have large (n, α) cross sections. Conversely, if the track detectors are doped with known quantities of these elements, they form convenient neutron dosimeters (*26, 29–31*).

Figure 8 shows how a simple material such as a glass microscope slide can be used to measure neutron dose over more than 4 orders of magnitude of neutron flux (*31*). The density of fission tracks is compared with the time the glass spent at a given position in the Brookhaven graphite reactor; the relation is linear. By separate radio-

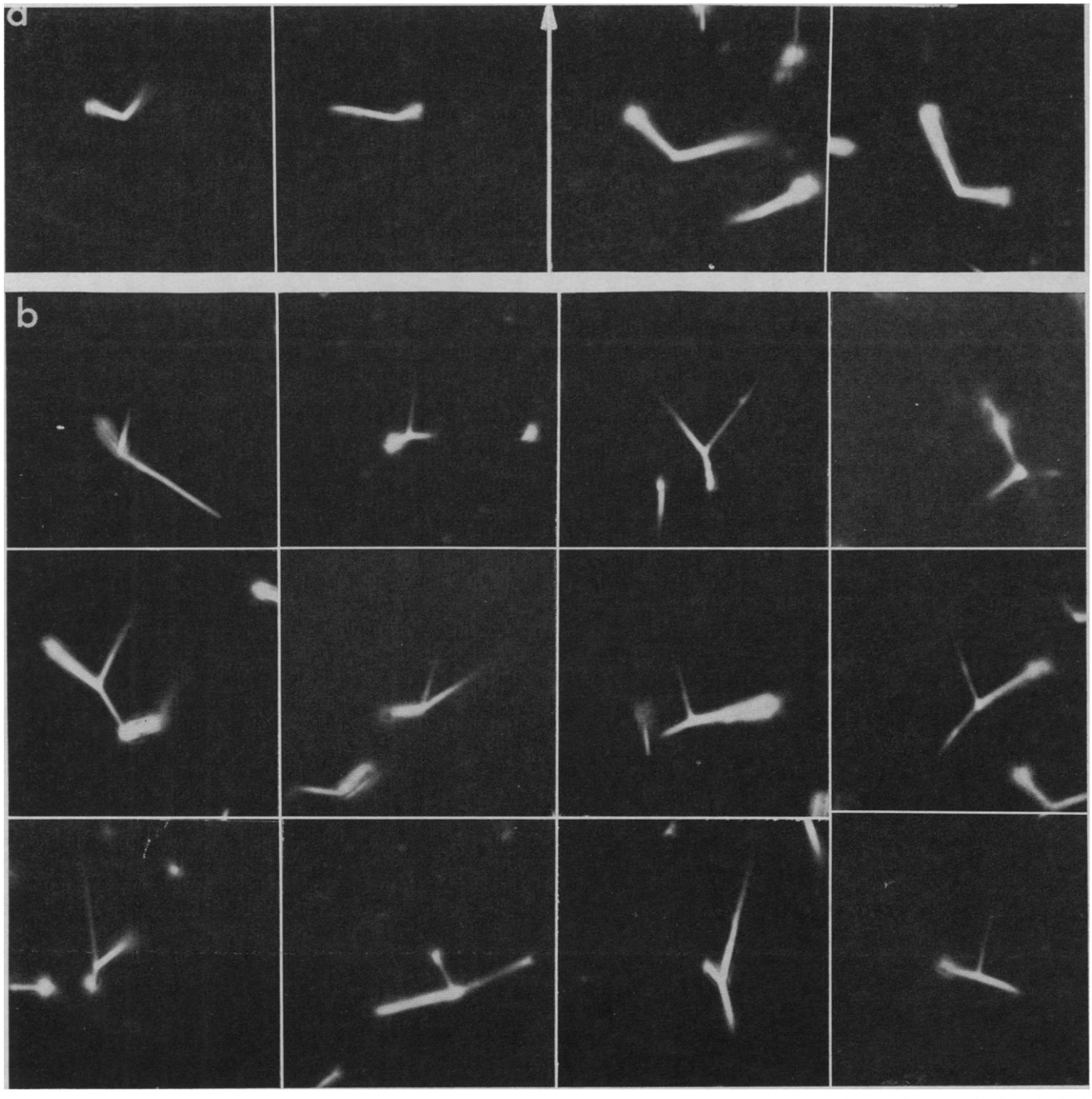

Fig. 6. Nuclear interaction of 400-Mev argon ions with thorium nuclei in a crystal of thorite ($ThSiO_4$), photographed with dark-field illumination after etching for 1 minute in boiling H_3PO_4 at 250°C. The argon ions, which do not register tracks, entered the crystal at a grazing angle of 15 degrees along the arrow. The V-tracks in *a* are binary fissions, whereas the three-pronged tracks in *b* are probably ternary fissions in which each fragment is sufficiently massive to register a track.

chemical measurements a calibration was made to determine the relation between the integrated flux and the track density (ρ_1). The result for this dosimeter is $\phi = 2.6 \times 10^{11}\rho_1$. Although the scatter in the data is appreciable, it is less than that encountered with conventional radiochemical techniques during the same experiments. When materials of low uranium content are selected, doses of 10^{20} or more thermal neutrons per square centimeter can be measured (*30*); with materials of high uranium content one can detect as few as a hundred thermal neutrons (*26*).

To measure the uranium, plutonium, boron, or lithium content of a sample it is not necessary that the sample itself register charged-particle tracks. Instead, the sample is simply placed next to a track-detecting material during neutron irradiation. The detector then receives fission fragments or heavy-particle decay products from the surface layers of the sample being analyzed. Figure 9 (left and right) gives examples of such detection experiments in which plastic detectors, which are sensitive respectively to α-particles and to fission fragments, are used. Figure 9 (left) shows the boron distribution in a metal alloy (*32*); the nonuniform distribution of α-particle tracks shows that the boron is clustered and not in solid solution. Figure 9 (right) shows the distribution of uranium in a fossil antelope bone sent us by K. P. Oakley of the British Museum (*33*). Here the distribution is random, and the concentration is easily measured by counting tracks.

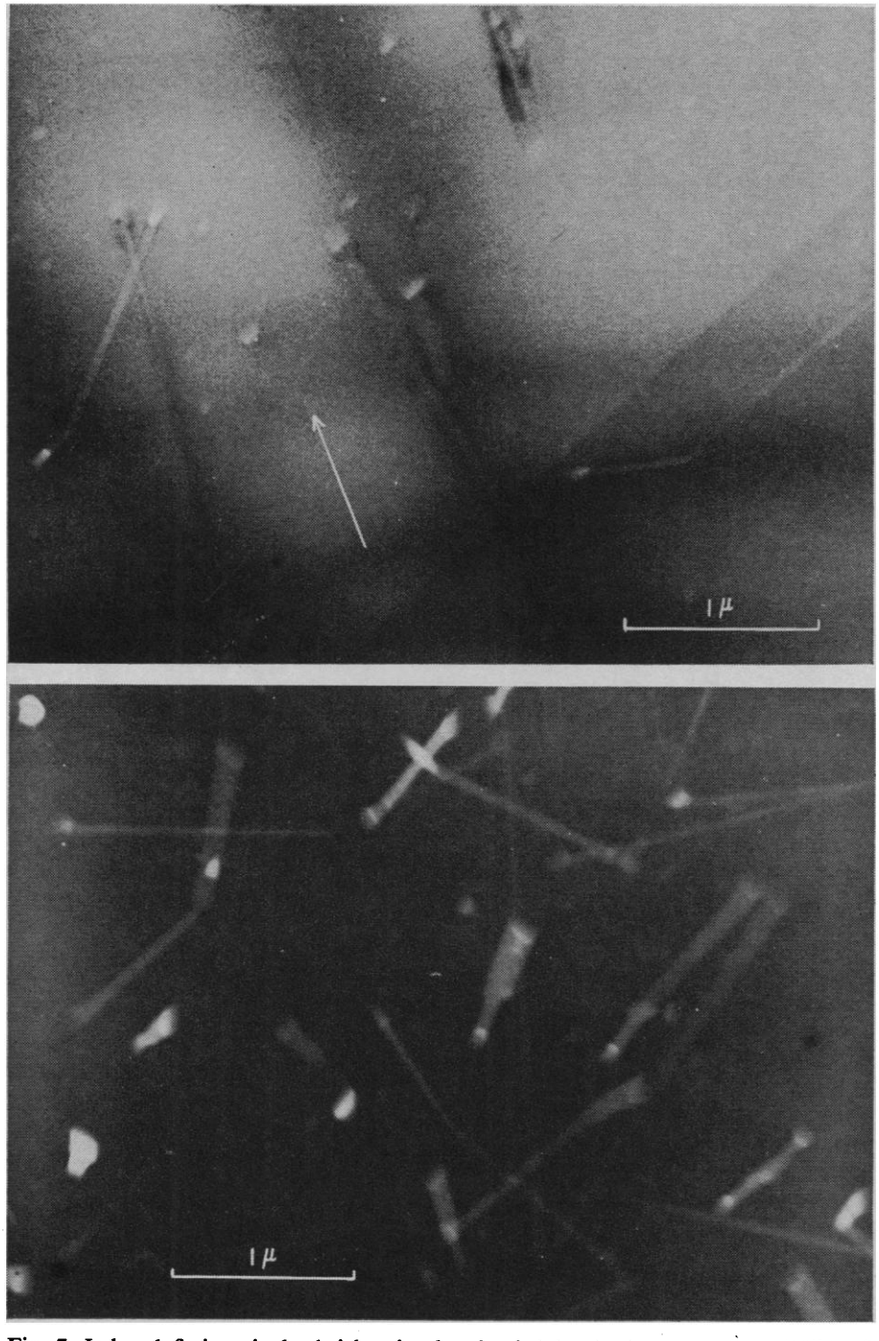

Fig. 7. Induced fissions in lead-rich mica bombarded by (top) oxygen ions (10^{12}/cm^2) that entered the crystal along the direction indicated by the arrow, and by (bottom) 3-Gev protons (5×10^{15}/cm^2) normal to the crystal. Each bent track represents the fission of a lead nucleus that was moving as a result of a collision. The absence of a visible tail at the vertex of a V-track is taken as evidence that the nucleus fissioned less than 5×10^{-16} second after collision with the proton.

With these methods it is possible to measure the uranium content and distribution in extremely minute samples of practically any material. With Ursula B. Marvin of the Smithsonian Astrophysical Observatory, we are studying the fractionation of uranium among the various mineral phases of meteorites which are noted for their small average uranium contents. In the first meteorite we have studied (*34*)—the Vaca Muerta mesosiderite—we find uranium concentrations that range from ~4000 parts per million (by weight) in the rare, minute zircon grains (*35*) down to less than 10^{-3} part per million in certain feldspar crystals. To the radiochemist who deduces a radioactive-decay age from the measured uranium content of a "representative" bulk sample and the lead content of a similar sample from the same meteorite, these results point out a possible source of considerable error.

Filters: Applications to Separation of Biological Cells

Studies of charged-particle tracks have led to the development of a new filter that is useful for biological studies. Consider a material in which we can etch long, narrow, charged-particle tracks. If we irradiate a thin sheet with a collimated beam of fission fragments, we can produce a controlled number of tracks which are perpendicular to the sheet. Next we etch holes through the sheet and adjust their size by specifying the etching time. Holes ranging from ~50 Å up to many microns in diameter are easily attainable (*36*). Figure 10 shows a mica

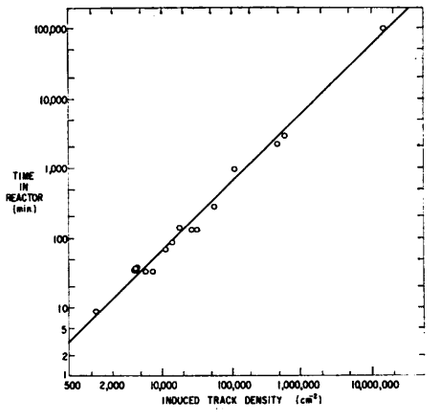

Fig. 8. Densities of induced fission tracks, as counted in a glass dosimeter, plotted against time spent in the reactor. The linear increase in the track density with time spent in the reactor may be converted to a direct measure of the integrated neutron flux (*31*).

sheet containing holes with very uniform diameters (~700 Å). Similar etched mica sieves are being used by C. P. Bean of our laboratory as simulated biological membranes in ionic-transport studies (*37*).

The polycarbonate plastic is a convenient material in which to produce holes from 1 micron to 15 or 20 microns in diameter (*38*)—a size range which includes sizes of typical biological cells. Such filters are appropriate for separating biological cells of different sizes. An example of such an application is the use of such filters to separate free-floating cancer cells from blood (*39*). Figure 11 shows a result of such a filtration experiment at our laboratory: the cancer cells, which were larger than the holes, were caught and then stained *in situ*.

Geochronology, Archeology, Prehistory

Perhaps the most exciting aspect of the fission tracks arises in the examination of natural materials (*40*) such as are shown in Fig. 12. These samples contain fission tracks, and yet the samples were not irradiated by man. Instead, these tracks are the result of trace uranium impurities, some of which spontaneously fissioned during geological time, creating in this way a record of the age of the samples. [Although most uranium atoms decay by alpha emission, about one in every 2 million atoms decays by spontaneous fission, the fission-decay constant being $\sim 10^{-16}$/year (*22*).] Since the density ρ_s of these spontaneous-fission tracks increases with the uranium concentration and the age of the sample, we can count the tracks, measure the uranium content (by inducing fission in a nuclear reactor, as described earlier), and then calculate the age (*41*). Quantitatively, the age A is found from the equation

$$\rho_s/\rho_i = [\exp(\lambda_D A) - 1](\lambda_F/\lambda_D f) \qquad (1)$$

where λ_F and λ_D are the spontaneous-fission and total-decay constants of U^{238}, f is the fraction of the total uranium fissioned in the reactor irradiation that was used to measure the uranium content, and ρ_i is the new density of tracks induced by this irradiation. A basic assumption of this method is that fission tracks can be stored over long time spans. The validity of this assumption is supported by the results of the laboratory annealing experiments described above. Extrapolation of these laboratory experiments (*15*, *16*) leads us to conclude that in some materials tracks can be stored at temperatures below ~600°C for times equal to the age of the solar system.

The fission-track dating method has now been tested and shown to be applicable for dating a wide variety of materials over a time range which spans more than 9 orders of magnitude (*5*, *15*, *22*, *42–48*). Figure 13 shows a comparison of fission-track ages and ages known either absolutely or by other dating methods. It may be seen that, for times of less than 10^8 years, ages obtained by the fission-track method are generally in accord with ages determined by other methods (though there are occasional discordances for individual samples) and that, for very long times, the determinations are less frequently in accord. Even for the very long times there are enough cases of agreement to establish the basic validity of the method. As in all age measurements, one must ask what time interval is being measured. It is our opinion that the "low" ages which are sometimes obtained by the fission-track method represent definite physical events, such as heating episodes. Such discrepancies due to heating, if found within the various members of a group of associated minerals, provide a way of measuring the date and extent of thermal events (*15*).

The critical quantity which determines the time span over which a given material can be dated is the uranium content. A concentration of 1 part per million is sufficient to make an object more than 500,000 years old easily datable. Since this is a common uranium concentration in nature,

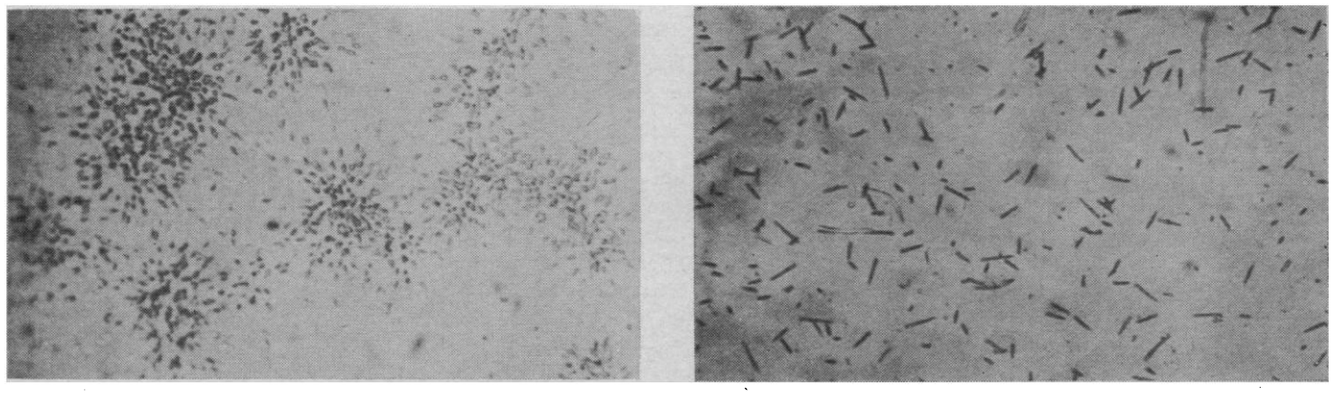

Fig. 9. Microchemical analysis of materials. (Left) Alpha-particle tracks in a plastic sheet show that boron atoms were nonhomogeneously distributed within the Nb_3Al alloy. The sheet was pressed against a polished surface of the alloy during neutron irradiation (*32*). (Right) Tracks of a uranium fission fragment, from a fossil antelope bone from Hopefield (Elandsfontein), Cape Province, South Africa. The uranium is uniform and present in a concentration of 18 parts per million, as determined by a count of the induced fission tracks. Specimens weighing as little as 20 micrograms may be easily used. [Sample loaned by K. P. Oakley of the British Museum (*33*)]

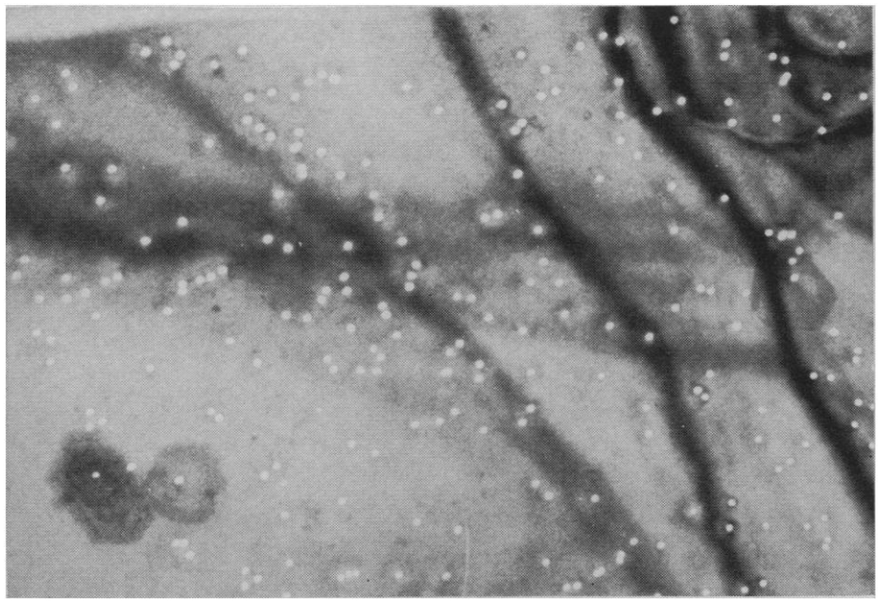

Fig. 10. A mica sieve. The hole density of $5 \times 10^8/cm^2$ and the hole diameters of 700 Å were produced by fission-fragment irradiation normal to this thin sheet, followed by etching to the desired hole size (*36*).

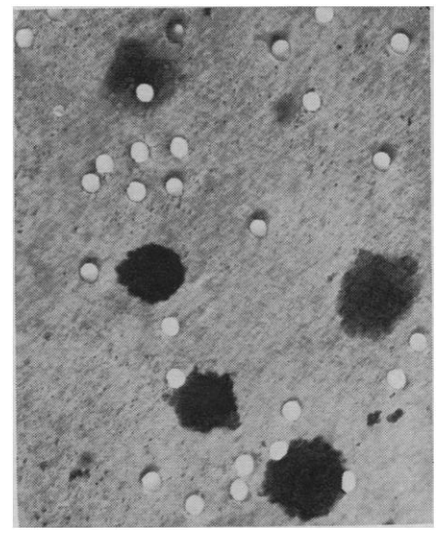

Fig. 11. Filtration of cancer cells by means of a plastic sieve. The holes have been etched to a diameter of 5 microns; holes of this size allow blood cells to pass though but catch most cancer cells. The cells have been stained and appear as irregular shapes. The fission-track holes are circular (*61*).

times of geological interest are readily ascertainable, as the many experimental points at the right of Fig. 13 indicate. By selecting minerals of higher uranium content, such as zircon (*45*), apatite (*5*), and some volcanic glasses (*42, 46, 48*), we can examine the whole of the Pleistocene; an age of about 4000 years has, for example, been measured on one piece of obsidian (*48*). Progressing still higher in uranium content, we can date man-made glass if we select objects to which uranium has been deliberately added. One such object we have dated, in work with R. H. Brill of the Corning Museum of Glass (*44*), is a 19th century candlestick containing 0.6 percent uranium trioxide. We have also shown that some ancient glasses contain enough uranium to give useful archeological information on ages (*49*).

The origin and history of tektites are problems which have long plagued and fascinated scientists of diverse disciplines. These small glass objects have passed downward through the earth's atmosphere at hypersonic velocities and have landed on certain limited areas of the earth. Studies with both potassium-argon and fission-track dating have shown that the tektites strewn within each of four large continental areas have four distinct ages (*15, 42, 47, 50*). Dating of the thin flange of glass which was remelted during entry of some of these tektites into the atmosphere has shown that the time of arrival on earth is not measurably different from the time of original solidification (*42*). A search for cosmic-ray-induced tracks has shown that tektites spent less than 300 years in space, on the average (*51*). And finally, dating —again by both the potassium-argon and the fission-track methods (*15, 42, 47, 52*)—has shown that other bodies, massive enough to melt terrestrial material to form glass (and in some cases to create craters several kilometers in diameter), impacted on the earth at, apparently, the times of the tektite falls. As yet there is no agreement on how these bodies came into existence or on how they are connected with the tektites.

An application of fission-track dating to prehistory is the dating of volcanic glass from Bed I of the Olduvai Gorge, Tanganyika, the site of the finds (*53*), by L. S. B. Leakey and M. D. Leakey, of two varieties of hominid remains, *Zinjanthropus* and *Homo habilis*. Since the age of 1.8 million years obtained by Leakey, Evernden, and Curtis (*54*) by the potassium-argon method for anorthoclase from Bed I has been questioned (*55*), we measured, in collaboration with Leakey, the age of the volcanic pumice in Bed I. The result was a value of 2.03 ± 0.28 million years (*46*), in agreement with the previous determination.

It is important to note that the possible sources of error in the potas-

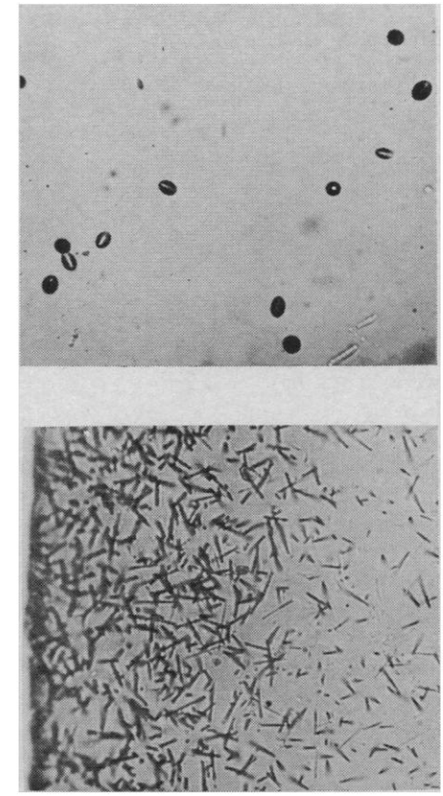

Fig. 12. Natural tracks in terrestrial materials: (Top) Volcanic glass, Macusanite, from Peru (etched for 10 seconds in 48-percent hydrofluoric acid); (bottom) a zircon crystal from Australia (etched for 1 minute in boiling phosphoric acid at 500°C). The increase in track density as the free surface of the zircon is approached indicates that a nonuniform uranium distribution existed in the past.

sium-argon and fission-track methods are different. For example, the presence of inherited argon in the anorthoclase, which, with the potassium-argon method, would lead to too high an age value, would not affect fission-track dating. On the other hand, apparent ages obtained by the fission-track method more often deviate from true ages as a result of heating episodes, which make the apparent age too low. The fact that ages obtained by the two methods agree within the precision of the experimental procedures is therefore strong support for the validity of an age of nearly 2 million years. A second inference which can be drawn from the two dating results for Bed I has to do with the duration of the Pleistocene (*46*). The position of Bed I in the stratigraphic sequence implies that the Pleistocene must have started considerably more than 2 million years ago and suggests a value of about 3 million years ago as a reasonable estimate.

Meteorites and Cosmic Rays

Our work on tracks in solids started with the idea that natural samples might contain naturally occurring tracks which could be used to obtain information about the radiation history of the samples. The original idea was to search for tracks of cosmic-ray origin in extraterrestrial materials. Although it happened that naturally occurring tracks—or "fossil" tracks—were first found in terrestrial samples, in which the contribution from cosmic rays can be shown to be negligible, cosmic-ray tracks have now been seen in meteorites, the first observations having been made (*56*) in collaboration with M. Maurette of the University of Paris and P. Pellas of the Paris Museum.

Meteorites, because of their extreme antiquity ($\sim 4.5 \times 10^9$ years) (*57*) and their long exposures to cosmic rays ($\sim 10^6$ to 10^9 years) (*57*), contain a wealth of information about the early history of the solar system and about the cosmic radiation. We are beginning to extract some of this information by studying fossil particle tracks in meteoritic minerals having different uranium concentrations. From the measured values of dE/dx listed in Table 1, we calculate that tracks in extraterrestrial materials can be formed in five ways: through (i) spontaneous fission of U^{238} or Pu^{244}; (ii) cosmic-ray-induced fission of heavy elements such as lead, thorium, and uranium; (iii) fission of U^{235} by slowed-down neutrons from cosmic-ray interactions in the material; (iv) recoil of nuclei in cosmic-ray-induced spallation reactions; and (v) bombardment with very heavy, slowed-down cosmic-ray primaries.

Fortunately, tracks from most of these sources have distinctive identify-

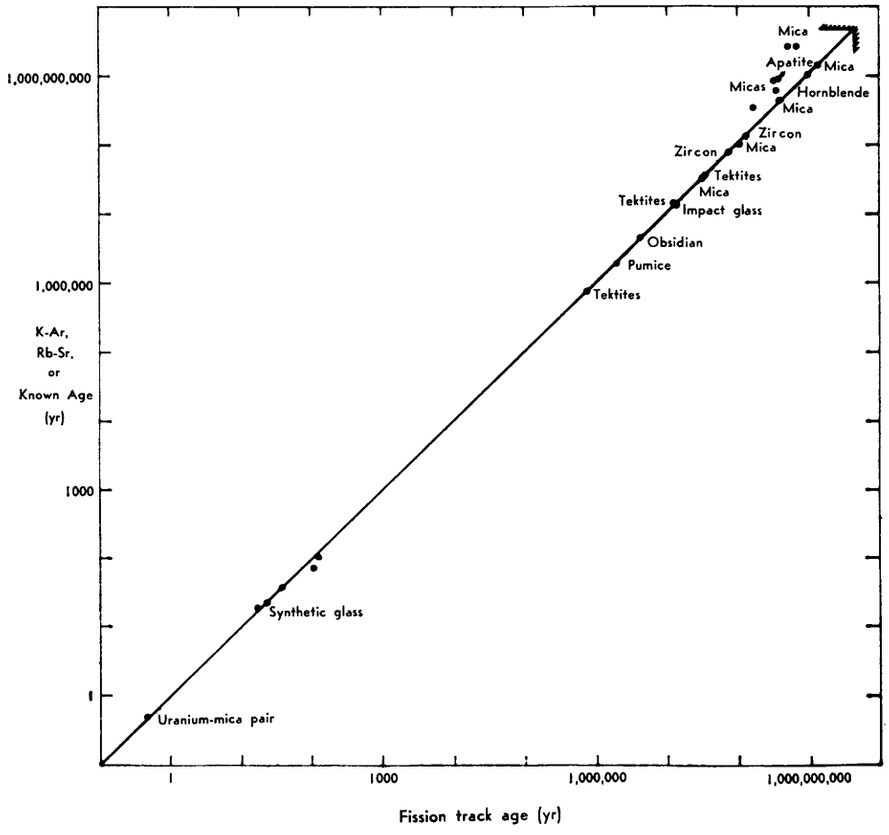

Fig. 13. Comparison of ages found by fission-track dating with those established by other means. The samples less than 200 years old are man-made; the older ones are geological.

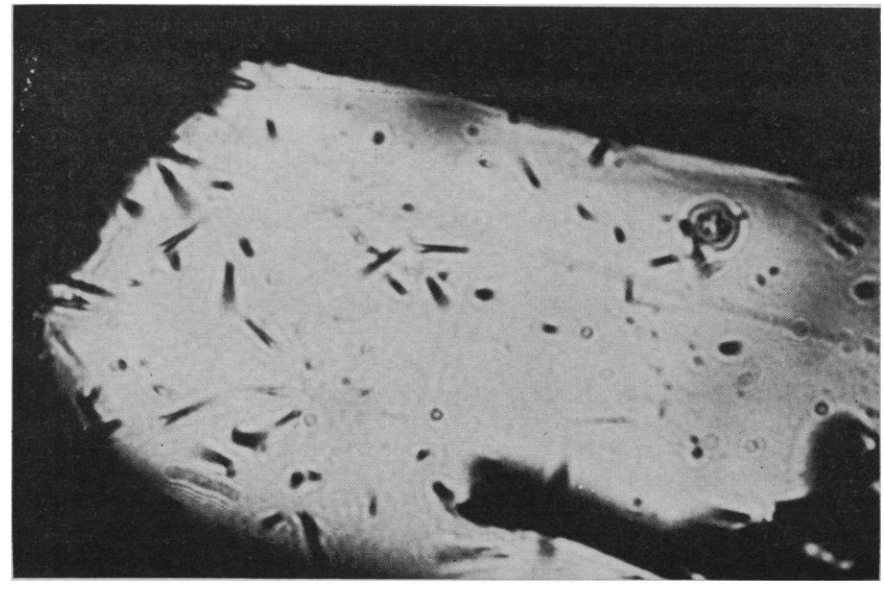

Fig. 14. Fossil tracks of cosmic-ray primaries, with atomic number between ~20 and ~28, in a bronzite grain (40 by 60 μ) from a chondrule in the Clovis meteorite.

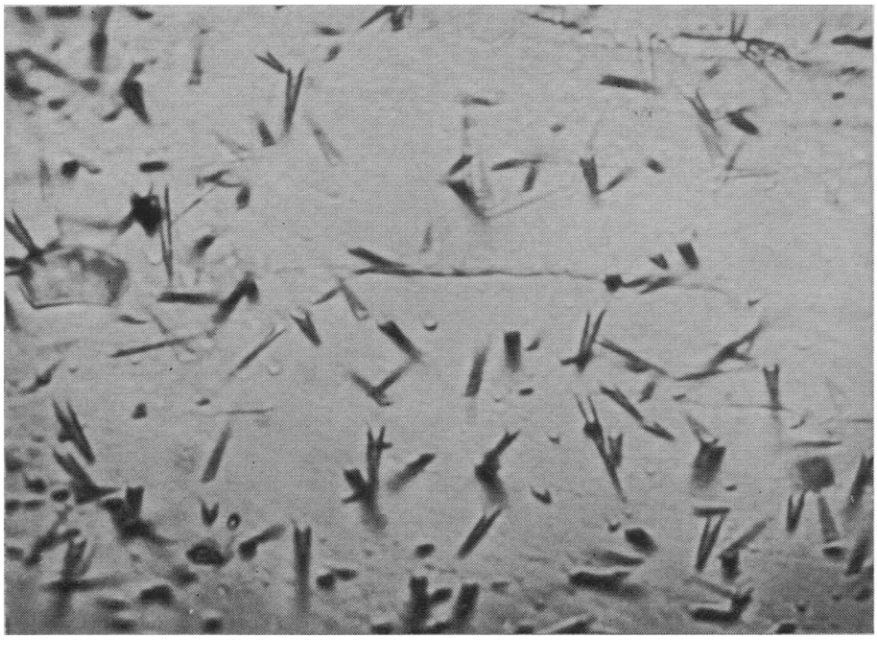

Fig. 15. Fossil tracks in a diopside crystal from the iron meteorite Odessa. The crystal, which measured about 0.3 by 0.2 by 0.1 millimeter, was etched for 10 minutes in NaOH solution at 200°C. We have deduced that about 98 percent of the tracks in the micrograph resulted from spontaneous fission of Pu^{244}.

ing characteristics and vary in relative number with different measurable parameters, such as the uranium content and the $(dE/dx)_c$ of the mineral, as well as the location of the mineral inside the meteorite. Tracks of different origin can thus be separated one from the other, each contributing different information.

Calibration experiments with 3-Gev protons, made in collaboration with G. Morgan of the Brookhaven Cosmotron Staff, have shown that in most meteoritic minerals spallation recoils and high-energy-induced fission events contribute a negligible number of background tracks. Thus, though protons are the dominant particles in the primary radiation, they are not responsible for the bulk of the tracks found in meteorites.

Very heavy cosmic rays, such as iron nuclei, though much less abundant than protons and α-particles, bombard the surfaces of meteorites at the rate of $\sim 10^5$ cm^{-2} yr^{-1} and can form etchable tracks as they near the end of their range. These tracks are characterized by a large variation in density with depth, by a marked variation in average length in materials with different $(dE/dx)_c$, and by a maximum track length, in a given mineral, that increases rapidly with mass. The pronounced variation in density with depth arises both from the high dE/dx of heavy cosmic rays and from their short nuclear-interaction mean free paths. We have now identified heavy cosmic-ray tracks in a number of stony and stony-iron meteorites. Figure 14 shows such tracks in a single grain of a polished thin section from the Clovis chondrite. If the duration of exposure of a meteorite to cosmic rays is known, the depth of a sample below the original pre-atmospheric surface can be deduced from the density of such heavy-particle tracks.

From length measurements of heavy cosmic-ray tracks in meteoritic crystals, we are studying the now unknown abundances, in the cosmic radiation, of heavy elements of atomic number higher than that of iron. We are also attempting to measure these abundances in the present-day cosmic-ray flux by flying special plastic detectors in balloons and satellites.

Some months ago it occurred to us that if meteoritic minerals crystallized and cooled shortly after the condensation of the solar system, then they might contain large numbers of tracks from spontaneous fission of fissionable elements that are now extinct because of their short half-lives. Plutonium-244 is the extinct isotope most likely to have left fossil tracks. Even though its half-life, 7.6×10^7 years, is much shorter than that of U^{238}, it spontaneously fissions with a frequency 4×10^5 times the rate for U^{238}, so that its contribution to the total density of spontaneous-fission tracks in a meteoritic crystal might rival or exceed that of U^{238}. In fact, if the fossil-track density measured in a particular crystal is simply the sum of two spontaneous-fission-track densities, $\rho_U + \rho_{Pu}$, then the time interval, ΔT, between the end of element formation and the cooling-down of that crystal can be calculated from the following expression (*59*):

$$\frac{\rho_{Pu}}{\rho_U} = \left(\frac{Pu^{244}}{U^{238}}\right) \exp\left[-(\lambda_{DPu} - \lambda_{DU})\,\Delta T\right] \frac{\lambda_{FPu}\,\lambda_{DU}\,[1 - \exp(-\lambda_{DPu} T)]}{\lambda_{DPu}\,\lambda_{FU}\,[1 - \exp(-\lambda_{DU} T)]} \quad (2)$$

where the λ's are spontaneous-fission and total-decay constants for Pu^{244} and U^{238}. If we take the abundance ratio $(Pu^{244}/U^{238}) = 1/45$ at the end of nucleosynthesis (*60*), and if $T = 4.5 \times 10^9$ years (*57*), then we have the simple relation

$$\Delta T \text{ (in units of } 10^6 \text{ yr)} = 112 \ln (306\, \rho_C/\rho_{Pu}). \quad (3)$$

Provided a sample from more than ~20 centimeters below the surface of a meteorite is studied, the contribution from heavy cosmic-ray primaries is negligibly small. We have now counted fossil fission tracks (identified by their characteristic length distribution) in deeply buried crystals from several very large iron meteorites and find that the observed number is many times greater than the number expected from the U^{238} concentration and an assumed age of 4.5×10^9 years. Figure 15 shows fossil fission tracks in a diopside crystal that was removed from the huge iron meteorite Odessa. Only 2 percent of the tracks seen in Fig. 15 came from spontaneous fission of U^{238}. In a separate publication (*59*) we have given detailed arguments to show that fission of extinct Pu^{244} is the most reasonable explanation for the other 98 percent. The cooling time for Odessa, calculated from data given in reference *3*, is 2×10^8 years.

Future Work

Much work remains to be done in the study and application of particle-track registration in solids. For example, the discovery that charged particles produce latent images of tracks in most insulating solids provides a strong incentive to develop additional techniques for revealing these tracks. The study of short-time decay events by means of the electron microscope

has been mentioned, as has the possibility of studying various heavy-ion interactions, in both terrestrial and extraterrestrial samples. Study of the latter could also conceivably lead to the discovery of new types of charged particles, such as magnetic monopoles.

One of the most intriguing possibilities for future work is the study of fossil tracks in lunar material—when it becomes available. Provided adequate samples of insulating materials (at least 50 microns on a side) are found, track studies should give a wealth of information concerning a number of questions of interest, such as the rate of lunar erosion (or accretion), the age at which the moon solidified, the date of impacts or eruptions on the surface, and the abundance of very heavy primaries in the cosmic radiation.

Summary

Heavy charged particles create narrow damage trails in many solids. The display of such tracks by preferential chemical etching has provided useful tools in many areas of endeavor: solid-state track detectors for nuclear physics, neutron dosimeters for nuclear engineering, a new means of performing chemical microanalysis of certain elements, filters capable of separating different biological cells, a method of dating geological and anthropological materials, and a means of examining the history and space environment of extraterrestrial objects.

References and Notes

1. E. C. H. Silk and R. S. Barnes, *Phil. Mag.* **4**, 970 (1959).
2. The zircon crystal was thinned from a bulk sample by our colleagues D. J. Barber and N. J. Tighe at the National Bureau of Standards, using an etch of H_3PO_4 at 470°C.
3. G. Bonfiglioli, A. Ferro, A. Mojoni, *J. Appl. Phys.* **32**, 2499 (1961); K. Izui and F. E. Fujita, *J. Phys. Soc. Japan* **16**, 1779 (1961); P. B. Price and R. M. Walker, *J. Appl. Phys.* **33**, 3400 (1962); A. D. Whapham and M. J. Makin, *Phil. Mag.* **7**, 1441 (19(→ L. T. Chadderton and H. M. Montague-Pollock, *Proc. Roy. Soc. London Ser. A* **274**, 239 (1963); L. T. Chadderton and I. MacTevens, *Nature* **203**, 387 (1964).
4. P. B. Price and R. M. Walker, *J. Appl. Phys.* **33**, 3407 (1962).
5. R. L. Fleischer and P. B. Price, *Geochim. Cosmochim. Acta* **28**, 1705 (1964).
6. ———, *J. Appl. Phys.* **34**, 2903 (1963).
7. ———, *Science* **140**, 1221 (1963).
8. P. B. Price and R. M. Walker, *Phys. Letters* **3**, 113 (1962).
9. Under favorable conditions it is possible to resolve etched tracks with diameters as small as 500 Å by dark-field illumination.
10. D. A. Young, *Nature* **182**, 375 (1958).
11. The geometry of track etching is discussed in more detail by R. L. Fleischer and P. B. Price in *J. Geophys. Res.* **69**, 331 (1964).
12. C. Childs and L. Slifkin, *IEEE (Inst. Electron. Elec. Engrs.) Trans. Nucl. Sci.* **9**, 134 (1962).
13. R. L. Fleischer, P. B. Price, R. M. Walker, E. L. Hubbard, *Phys. Rev.* **133A**, 1443 (1964).
14. The deuteron bombardments were performed by A. Borden, C. Porterfield, and R. Ritter of the University of Virginia.
15. R. L. Fleischer and P. B. Price, *J. Geophys. Res.* **69**, 331 (1964).
16. ——— and R. M. Walker, *ibid.* **70**, 1497 (1965).
17. J. A. Brinkman, *J. Appl. Phys.* **25**, 961 (1954).
18. F. Seitz, *Discussions Faraday Soc.* **5**, 271 (1949).
19. R. L. Fleischer, P. B. Price, R. M. Walker, *J. Appl. Phys.*, in press.
20. D. S. Burnett, R. C. Gatti, F. Plasil, P. B. Price, W. J. Swiatecki, S. G. Thompson, *Phys. Rev.* **134**, B952 (1964); S. G. Thompson, private communication.
21. G. N. Flerov, Yu. T. Oganesyan, Yu. V. Lobanov, V. I. Kuznetsov, V. A. Druin, V. P. Perelygin, K. A. Gavrilov, S. P. Tretiakova, V. M. Plotko, *Phys. Letters* **13**, 73 (1964).
22. R. L. Fleischer and P. B. Price, *Phys. Rev.* **133**, B63 (1964).
23. Synthetic thorite crystals were generously donated to us by G. W. Clark, Oak Ridge National Laboratory. See C. B. Finch, L. A. Harris, G. W. Clark, *Am. Mineralogist* **49**, 782 (1964).
24. W. J. Swiatecki, in *Second UN Geneva Conference on Peaceful Uses of Atomic Energy* (Pergamon, London, 1960), paper P/651.
25. For a preliminary account of our earlier work, see P. B. Price, R. L. Fleischer, R. M. Walker, E. L. Hubbard, in *Proceedings of Third Conference on Reactions between Complex Nuclei* (Univ. of California Press, Berkeley, 1963), p. 332.
26. R. M. Walker, P. B. Price, R. L. Fleischer, *Appl. Phys. Letters* **3**, 28 (1963).
27. J. Mory, in *Proceedings 5th International Conference on Nuclear Photography* (CERN, 1964).
28. P. B. Price and R. M. Walker, *Appl. Phys. Letters* **2**, 23 (1963).
29. M. Debeauvais, M. Maurette, J. Mory, R. M. Walker, *Inst. J. Appl. Radiation and Isotopes* **15**, 289 (1964).
30. P. Prevo, R. E. Dahl, H. H. Yoshikawa, *J. Appl. Phys.* **35**, 2636 (1964).
31. R. L. Fleischer, P. B. Price, R. M. Walker, *J. Nucl. Sci. Eng.* **22**, 153 (1965).
32. C. P. Bean, R. L. Fleischer, P. S. Swartz, H. R. Hart, G. E. Nichols, in preparation.
33. R. L. Fleischer, P. B. Price, R. M. Walker, paper presented at the International Glass Congress, Brussels, 1965 (G.E. Rept. No. 65-RL-3878M), in press.
34. R. L. Fleischer, C. W. Naeser, P. B. Price, R. M. Walker, U. B. Marvin, *Science* **148**, 629 (1965).
→ U. B. Marvin and C. Klein, Jr., *ibid.* **146**, 919 (1964).
36. R. L. Fleischer, P. B. Price, R. M. Walker, *Rev. Sci. Instr.* **34**, 510 (1963).
37. A preliminary account, by C. P. Bean, M. V. Doyle, and G. Entine, is in preparation.
38. R. L. Fleischer, P. B. Price, E. M. Symes, *Science* **143**, 249 (1964).
39. S. H. Seal, *Cancer* **17**, 637 (1964).
40. P. B. Price and R. M. Walker, *Nature* **196**, 732 (1962).
41. ———, *J. Geophys. Res.* **68**, 4847 (1963).
42. R. L. Fleischer and P. B. Price, *Geochim. Cosmochim. Acta* **28**, 755 (1964).
4 → ———, E. M. Symes, D. S. Miller, *Science* **143**, 349 (1964); M. Maurette, P. Pellas, R. M. Walker, *Bull. Soc. Franc. Mineral. Crist.* **87**, 6 (1964).
44. R. H. Brill, R. L. Fleischer, P. B. Price, R. M. Walker, *J. Glass Studies* **6**, 151 (1964).
45. R. L. Fleischer, P. B. Price, R. M. Walker, *J. Geophys. Res.* **69**, 4885 (1964).
4 → ——— and L. S. B. Leakey, *Science* **148**, 72 (1965).
47. R. L. Fleischer, P. B. Price, R. M. Walker, *Geochim. Cosmochim. Acta* **29**, 161 (1965).
48. R. L. Fleischer, P. B. Price, R. M. Walker, L. S. B. Leakey, *Nature* **202**, 1138 (1965).
49. R. L. Fleischer and P. B. Price, *Science* **144**, 841 (1964).
50. J. Zähringer, in "Radioactive dating," *Publ. Intern. Atomic Energy Agency Vienna* (1963), p. 289.
51. R. L. Fleischer, C. W. Naeser, P. B. Price, R. M. Walker, M. Maurette, *J. Geophys. Res.* **70**, 1491 (1965).
52. W. H. Gentner, J. Lippolt, O. A. Schaeffer, *Geochim. Cosmochim. Acta* **27**, 191 (1963); W. H. Gentner, J. Lippolt, O. Müller, Z. *Naturforsch.* **19a**, 150 (1964).
53. L. S. B. Leakey, *Nature* **184**, 491 (1959); ——— and M. D. Leakey, *ibid.* **202**, 4 (1964).
54. L. S. B. Leakey, J. F. Evernden, G. H. Curtis, *ibid.* **191**, 478 (1961).
55. G. H. R. von Koenigswald, W. Gentner, H. J. Lippolt, *ibid.*, p. 720; W. L. Straus, Jr., and C. B. Hunt, *Science* **136**, 293 (1962).
56. M. Maurette, P. Pellas, R. M. Walker, *Nature* **204**, 821 (1964).
57. For a recent review of meteorite ages and cosmic-ray exposure times, see E. Anders, in *The Moon, Meteorites and Comets*, B. M. Middlehurst and G. P. Kuiper, Eds. (Univ. of Chicago Press, Chicago, 1963), p. 402.
58. P. B. Price and R. M. Walker, *Phys. Rev. Letters* **8**, 217 (1962); M. Maurette and R. M. Walker, *J. Phys. Radium* **25**, 43 (1964).
59. R. L. Fleischer, P. B. Price, R. M. Walker, *J. Geophys. Res.* **70**, 2703 (1965).
60. W. A. Fowler and F. Hoyle, *Ann. Phys.* **10**, 280 (1960); T. P. Kohman, *J. Chem. Educ.* **38**, 73 (1961).
61. Such filters, under the trade name Nuclepore, are manufactured by G.E. Irradiation Processing Operation, Pleasanton, Calif.
62. We are indebted to C. B. Moore, Arizona State University, for samples of the Moore County and Lafayette meteorites; to E. Olsen, Chicago Natural History Museum, for the silicate inclusions from the Odessa and Kodaikanal meteorites; to E. P. Henderson, U.S. National Museum, for the samples from the Four Corners, Linwood, and Clovis meteorites; to Ursula B. Marvin, Smithsonian Astrophysical Observatory, for the silicate inclusions from the Toluca meteorite; and to V. E. Barnes, University of Texas, for the sample of Macusanite volcanic glass.